This is a peer-reviewed, accepted author manuscript of the following research article: Zhao, Y., Yang, J., Faes, M. G. R., Bi, S., & Wang, Y. (2022). The sub-interval similarity: A general uncertainty quantification metric for both stochastic and interval model updating. *Mechanical Systems and Signal Processing*, *178*, [109319]. https://doi.org/10.1016/j.ymssp.2022.109319

The sub-interval similarity: A general uncertainty quantification metric for both stochastic and interval model updating

Yanlin Zhao[1,2,3], Jianhong Yang[1], Matthias G.R. Faes[4], Sifeng Bi[5, *], Yao Wang[6]

1 University of Science and Technology Beijing, School of Mechanical Engineering, Beijing, China
2 Shunde Graduate School, University of Science and Technology Beijing, Guangzhou, China
3 Beijing Key Laboratory of Lightweight Metal Forming, Beijing, 100083, China
4 TU Dortmund University, Chair for Reliability Engineering, Dortmund, Germany
5 University of Strathclyde, Department of Mechanical & Aerospace Engineering, Aerospace Centre of Excellence, Glasgow, UK
6 China Academy of Launch Vehicle Technology, Beijing, China

* Corresponding author: Sifeng Bi (sifeng.bi@strath.ac.uk)

Abstract: One of the key challenges of uncertainty analysis in model updating is the lack of experimental data. The definition of an appropriate uncertainty quantification metric, which is capable of measuring as sufficient as possible information from the limited and sparse experimental data, is significant for the outcome of model updating. This work is dedicated to the definition and investigation of a general-purpose uncertainty quantification metric based on the sub-interval similarity. The discrepancy between the model prediction and the experimental observation is measured in the form of intervals, instead of the common probabilistic distributions which require elaborate experimental data. An exhaustive definition of the similarity between intervals under different overlapping cases is proposed in this work. A sub-interval strategy is developed to compare the similarity considering not only the range of the intervals, but more importantly, the distributed positions of the available observation samples within the intervals. This sub-interval similarity metric is developed to be capable of different model updating frameworks, e.g. the stochastic Bayesian updating and the interval model updating. A simulated example employing the widely

known 3-dof mass-spring system is presented to perform both stochastic Bayesian updating and interval updating, to demonstrate the universality of the proposed sub-interval similarity metric. A practical experimental example is followed to demonstrate the feasibility of the proposed metric in practical application cases.

1 Introduction

Model updating has been developed as a classical but crucial technique to guarantee the trustfulness of numerical simulation by calibrating the numerical models and their parameters taking the experimental data as a reference. The increasing attention paid to uncertainty analysis during numerical modelling raises a tendency to extend updating strategies from the deterministic domain to the non-deterministic domain, e.g. the stochastic model updating and the interval model updating. This tendency, however, leads to a critical problem about how to quantify the uncertainty information based on massive numerical simulations but always limited experimental observations. This paper is hence dedicated to the development of a general-purpose Uncertainty Quantification (UQ) metric, which is applicable to a wide range of current updating procedures. This metric is based on the idea to divide the investigating intervals into a series of sub-intervals and assess the similarity among these sub-intervals. It will be elaborated as the Sub-interval Similarity (SIS) in the following context.

The deterministic model updating strategy [1,2] aims at estimating the explicit 'true' value of the updating parameters based on minimizing the discrepancy between the computed and measured modal properties. Considering that both the modelling and testing processes are exposed to inevitable uncertainties, it is natural to characterize the simulated and tested features by a multi-simulation-multi-test scenario, implying that the model updating also should be carried out in the non-deterministic sense. Recently, the non-deterministic model updating has gained substantial interest, and elaborate literature is available in this field. Those methods can be generally classified into two categories, namely the probabilistic and non-probabilistic approaches [3,4]. In this work, we focus on the stochastic model updating, which belongs to the probabilistic approach, and the

interval model updating, which is one of the most representative non-probabilistic approaches.

In the probabilistic approach, the output features and the input parameters of the numerical model are both assumed to follow probabilistic distributions. The objective of stochastic model updating is no longer to obtain a single value of the parameter minimizing the difference between the deterministic experiment and the model prediction, but rather to estimate distributions properties of the input parameters, which propagate through the numerical model and represent the outputs with similar distribution properties of the observations. Pioneering work on stochastic model updating is presented in the companion papers by Mottershead et al. [5,6], where the mean and variance of the input parameters are calibrated using an inverse Monte Carlo approach. Govers and Link [7] develop a stochastic updating approach taking the covariance matrix of the parameters as the objective. The perturbation approach is proposed by Khodaparast et al. [8] to calibrate the first and second statistical moments of the parameters taking the natural frequencies and mode shapes as output features.

Besides those statistical moment-based methods, Bayesian updating is another representative approach for stochastic model updating. The Bayesian approach formulates the updating problem as a process to transform the prior distribution of the parameters to the posterior distribution by using the experimental data and the probabilistic prediction error of the model. The fundamental work of Bayesian updating is proposed by Beck and Katafygiotis [9] and Kennedy and O'Hagan [10]. The Markov Chain Monte Carlo (MCMC) algorithm has a natural connection with the Bayesian updating because of its capacity to general random samples from the posterior distribution of the calibrating parameters [11,12]. As a result, the MCMC Bayesian updating approach plays an important role in the current development and application of stochastic model updating [13–16].

A representative stochastic model updating task has been presented in the recently launched NASA Optimization Challenge under Uncertainty [17]. This challenge problem requires to calibrate both the epistemic parameters (presented in intervals) and the aleatory parameters (under a distribution-free hypothesis) based on a set of limited and chaotic data sequences. To solve this challenge, a comprehensive UQ approach is required to capture the uncertainty information from

the existing data sequence, and an efficient updating algorithm is significant to calibrate the uncertainty model of both the aleatory and epistemic parameters, given an appropriate hypothesis of the preliminary distributions. There is a dedicated special issue published in the journal *Mechanical Systems and Signal Processing,* collecting contributions to solve this challenge. Among the proposed approaches, the approximated Bayesian updating [18] has been proved to be an element approach to define an efficient likelihood function to capture both aleatory and epistemic uncertainties. A staircase density function [19] is proposed to construct a distribution-free uncertainty model of the aleatory parameters. To deal with the very limited and chaotic data sequence, the empirical mode decomposition and Bhattacharyya distance [20] are employed to extract sufficient uncertainty information, which is the precondition of the updating process.

The above discussed stochastic updating approaches, no matter frequentist or Bayesian method, have a universal feature that they take the distribution properties as the updating objective, and hence it is important to define a statistical UQ metric to quantify the difference between the simulations and observations from the probabilistic point of view. Besides the deterministic geometry distance, i.e. the Euclidian distance, the statistical distances such as the Mahalanobis distance [21], the Bhattacharyya distance [22,23], and the Kullback-Leibler divergence [24] are drawing increasing attention in the current development of stochastic model updating. A potential weakness of the probabilistic approaches, however, is that they typically require elaborate data to precisely estimate the distribution or the statistical moments of the output features, leading to a high economic or computational cost. Alternatively, the non-probabilistic interval approaches have been introduced to release this challenge [25,26].

The interval model updating characterizes the uncertainties only by the bounds and the position of the intervals, which needs no distribution or moment information as what is required by the stochastic updating. The interval updating is performed as inverse identification for the bounds of model parameters, based on the interval quantification of the model outputs. This process relies on the accurate propagation of uncertainties in the form of intervals. However, for practical applications, the interval arithmetic operations are difficult to directly implement in uncertainties propagation.

The difficulty results from the decoupling of interval numbers taking place in interval element matrix assembly as well as in the final solution phase [27,28]. To overcome such inconvenience, Faes et al. propose a multivariate interval quantification approach [29,30] based on the concept of convex hull, which is capable of building an indirect map from the convex hull of the experimental samples to the parameter space. In the presence of high dimensional applications where high calculation cost is encountered, the perturbation method [8], or some surrogate models [31,32] are introduced to release the calculation burden. Also, recently, a dedicated Multilevel quasi Monte Carlo sampling method based on Cauchy random variables for interval propagation was introduced [33].

In this context, no matter stochastic or interval updating, they always rely on an efficient UQ metric, which is expected to be capable of quantifying both modelling and experimental uncertainties with acceptable calculation cost. The above discussed probabilistic moments and statistical distance metrics encounter obstacles that the experimental data is limited in practical applications. Alternatively, the interval-based UQ metrics, such as the above mentioned convex hull [29], the interval overlap ratio [34], the satisfaction degree of the interval [35], and the sum of the relative errors of interval bounds [32], have been developed in recent year.

The objective of this paper is to propose an interval-based UQ metric named as the Sub-interval Similarity (SIS). The SIS metric, on the one hand, makes full use of the superiority of the interval-based metric as to be applicable in the presence of limited and sparse experimental data; On the other hand, the SIS metric is capable of handling location dispersion features of the experimental samples, especially when the number of these samples is limited, by an adaptive algorithm to assign the sub-intervals within both intervals of the simulation and observation data. Another advantage of the proposed SIS metric is that it is developed to be a universal metric in not only the interval model updating but also the stochastic model updating strategies. The feasibility and efficiency of the SIS metric in both stochastic and interval updating are demonstrated in the 3-dof mass-spring example, where the stochastic updating and interval updating results are compared with two published references, respectively. An additional example employing practically measured data from a series

of nominally identical steel plates is provided to demonstrate the feasibility of the proposed SIS metric in practical updating applications.

2 UQ in model updating

2.1 Uncertainty characterization in modelling process

The numerical modelling process consists of three key components, including the input parameters $\mathbf{X} \in \mathbb{R}^{\mathbf{n_x}}$, the output features $\mathbf{Y} \in \mathbb{R}^{\mathbf{n_y}}$, and the model $f: x \to y,\ \mathbb{R}^{n_x} \mapsto \mathbb{R}^{n_y}$, which can be expressed as

$$\mathbf{Y} = f(\mathbf{X}), \tag{1}$$

where the model $f(\cdot)$ is developed in different forms such as functional relationships, finite element models, or implicit black-box models, according to the complexity of the physical system to be modelled.

The uncertainties can be involved in all the three components whereby the modelling uncertainty presents the approximations of the numerical model $f(\cdot)$, the parameter uncertainty presents the lack of knowledge or randomness of the input parameters $\mathbf{X}$. The uncertainties of the inputs propagate through the model to the output features, which is typically known as Uncertainty Propagation. As a result, the output features, on the one hand, present the uncertainties from the modelling and parameterization processes; on the other hand, the observations of the output features are inevitably influenced by the experimental uncertainty.

Assume that the experiment is repeated on a series of structure prototypes, and totally N_e sets of measurements are available. The experimental outputs $\mathbf{Y}_e \in \mathbb{R}^{N_e \times n_y}$ are presented as a matrix with the following structure

$$\mathbf{Y}_e = \left\{\mathbf{y}_1, \mathbf{y}_2, \dots, \mathbf{y}_{n_y}\right\} \tag{2}$$

where $\mathbf{y}_i = \left[y_{1,i}, y_{2,i}, \dots, y_{N_e,i}\right]^T, i = 1,2, \dots, n_y$; n_y is the number of features predicted by the model, e.g. different orders of natural frequencies or responses on different positions of the structure

system.

Similarly, considering there are N_s number of simulations repeated employing the numerical model $f(\cdot)$, and we can get the predicted outputs $\mathbf{Y}_s \in \mathbb{R}^{N_s \times n_y}$ with the similar structure as the experimental outputs as shown in Eq. (2). The only difference is that the number of rows of $\mathbf{Y}_s$ has been changed from N_e to N_s.

The task of uncertainty quantification in model updating is to measure the difference between $\mathbf{Y}_s$ and $\mathbf{Y}_e$ with the consideration of the uncertainty properties, such that to provide metrics to calibrate the input parameters $\mathbf{X}$, with the objective to tune the $\mathbf{Y}_s$ towards the $\mathbf{Y}_e$. It is hence important to select a suitable conception for UQ, i.e. the interval quantification or the probabilistic quantification, as it will be elaborated in the following subsection.

2.2 Interval quantification Vs. Probabilistic quantification

One of the classical UQ concepts is the probabilistic quantification which assumes or estimates a certain distribution to the output feature. The UQ process becomes the comparison of the distribution properties of the experimental and simulation output features. For example, the classical Euclidian distance $ED(\mathbf{Y}_e, \mathbf{Y}_s)$ provides a comparison of the means of two sets of data:

$$ED(\mathbf{Y}_e, \mathbf{Y}_s) = \left\{\sum_{i=1}^{n_y} \left[\mu_e^{(i)} - \mu_s^{(i)}\right]^2\right\}^{1/2}, \tag{3}$$

where $\mu^{(i)}$ is the mean of the *i*-th output feature estimated based on the experimental or simulated samples. Another statistical distance known as the Mahalanobis distance $MD(\mathbf{Y}_e, \mathbf{Y}_s)$ employs not only the mean but also the covariance to evaluate the difference

$$MD(\mathbf{Y}_e, \mathbf{Y}_s) = [(\bar{\mathbf{y}}_e - \bar{\mathbf{y}}_s)\mathbf{\Sigma}^{-1}(\bar{\mathbf{y}}_e - \bar{\mathbf{y}}_s)^T]^{1/2}, \tag{4}$$

where $\bar{\mathbf{y}}_e$ and $\bar{\mathbf{y}}_s$ are the mean vectors of $\mathbf{Y}_e$ and $\mathbf{Y}_s$, respectively; $\mathbf{\Sigma}^{-1}$ is the inverse of the covariance matrix.

There are other probabilistic UQ metrics employing directly the probabilistic distributions, e.g. the Kullback-Leibler divergence $KL(\mathbf{Y}_e, \mathbf{Y}_s)$ and the Bhattacharyya distance $BD(\mathbf{Y}_e, \mathbf{Y}_s)$:

$$KL(\mathbf{Y}_e, \mathbf{Y}_s) = \int_{\mathbb{Y}} P_e(y) \log \frac{P_s(y)}{P_e(y)} \mathrm{d}y \tag{5}$$

$$BD(\mathbf{Y}_e, \mathbf{Y}_s) = -\log \left\{ \int_{\mathbb{Y}} \sqrt{P_e(y) P_s(y)} \mathrm{d}y \right\} \tag{6}$$

where $P_e(y)$ and $P_s(y)$ are the Probabilistic Density Functions (PDF) of the experimental and simulated features. The above UQ metrics quantify the difference between two data sets considering the distribution properties. However, no matter the different orders of moments or the PDFs require a large number of data samples to provide a precise estimation of the distribution properties.

Alternatively, the interval quantification framework focuses on the range of the quantity of interest, and hence requires not as many data samples as the probabilistic quantification. Considering the intervals defined by the available experimental and simulated samples $I_e = \left[\underline{y}_e, \overline{y}_e\right]$, $I_s = \left[\underline{y}_s, \overline{y}_s\right]$. The interval UQ metric is defined based on the two key components of the interval, namely the length of the interval, $L(\mathbf{y}) = \overline{y} - \underline{y}$, and the position of the midpoint, $E(\mathbf{y}) = \frac{\overline{y}+\underline{y}}{2}$.

However, the interval UQ metric has an obvious drawback in that it neglects the randomness of the obtained experimental samples. Especially in the presence of irregular data, that is, an experimental sample is far from the majority of the existing samples. The length of the interval will be significantly governed by the irregular data, but the normal interval UQ metric will fail to quantify the weighting of the irregular experimental sample. The following section is consequently focusing on the UQ metric based on the sub-interval similarity which is capable of quantifying not only the range and position of the interval but also the sample location dispersion properties.

3 UQ metrics based on interval similarity

3.1 Interval similarity function

This section proposes a mathematical description of the relative position of two intervals. Consider two continuous intervals $A = \left[\underline{a}, \overline{a}\right]$ and $B = [\underline{b}, \overline{b}]$, first it is necessary to investigate different cases of the overlap between them, as illustrated in Fig. 1. The Relative Position Operator

(RPO) is defined using the length of the intervals, i.e. $L(A)$ and $L(B)$, according to different overlap cases:

$$\mathrm{RPO}(A,B)=\begin{cases}\dfrac{(\overline{a}-\underline{b})}{\max\{L(A),L(B)\}}, \text{Case1,2}\\ \dfrac{(\overline{a}-\underline{a})}{\max\{L(A),L(B)\}}, \text{Case3}\\ \dfrac{(\overline{b}-\underline{b})}{\max\{L(A),L(B)\}}, \text{Case4}\\ \dfrac{(\overline{b}-\underline{a})}{\max\{L(A),L(B)\}}, \text{Case5,6}\end{cases} \tag{7}$$

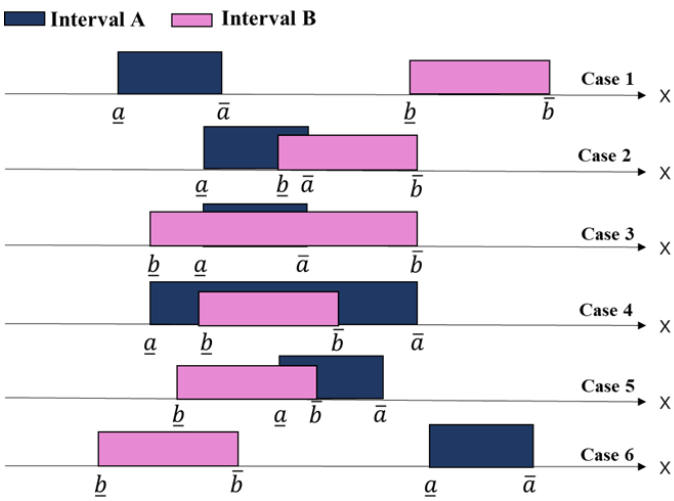

Fig. 1: Six cases of the overlap features of two intervals

As shown in Eq. (7), the denominators of the RPO of different cases are all the same as the maximum of the length of intervals A and B. For the numerator, when there is no overlap such as Cases 1 and 6, it is negative and its absolute value is determined as the shortest distance between these two intervals. When there is an overlap as shown in Cases 2-5, Eq. (7) defines the numerator as the length of the overlap block, and clearly this value is positive. As a summary, the value range of $\mathrm{RPO}(A,B)$ is determined as

$$\mathrm{RPO}(\mathrm{A},\mathrm{B}) \in (-\infty, 1]. \tag{8}$$

When intervals A and B are the same, $\mathrm{RPO}(\mathrm{A},\mathrm{B})$ reaches the maximum value one. A negative infinity of $\mathrm{RPO}(\mathrm{A},\mathrm{B})$ means the intervals A and B are infinitely far from each other with no overlap. An infinite value, however, would be insensitive to the calibrating parameters and hence leading the

model updating process prohibitive. Consequently, we construct the Interval Similarity Function (ISF) as

$$\mathrm{ISF}(A,B) = \frac{1}{1+\exp\{-\mathrm{RPO}(A,B)\}}. \tag{9}$$

As illustrated in Fig. 2, since $\mathrm{RPO(A,B)}$ falls within the range $(-\infty, 1]$, the value of $\mathrm{ISF}(A,B)$ is limited within (0, 0.7311]. The proposal of $\mathrm{ISF}(A,B)$ as a calibrating metric in model updating is beneficial because, on the one hand, the metric value is finite, and on the other hand, the metric has a high gradient as the value moves close to one, as shown in Fig. 2. Such a high gradient leads to a high sensitivity of the calibrating parameters especially when the parameters are close to the target values, which is good for convergence of the updating process.

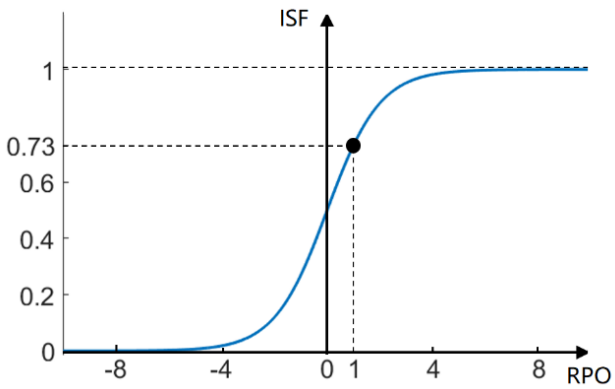

Fig. 2 Value range of the interval similarity function

3.2 Sub-interval similarity

The interval similarity function based on RPO provides a mathematical description of the discrepancy of two intervals, which can be employed as the parameter calibration metric in model updating. However, the RPO metric has an obvious drawback that its values is non-unique to some overlapping cases. Recal the different cases in Fig. 1 and consider another special case when the intervals A and B have a common bound, i.e., Interval A $[\underline{a}, X]$ and Interval B $[X, \overline{b}]$. Regardless the actual length of A and B, $\mathrm{RPO(A,B)}$ would always equal to 0. This means the RPO, for some cases, is insensitive to uncertainty, i.e. the length of the intervals.

This phenomenon is essentially because that RPO neglects the interval distributional feature of

the samples within the interval. This drawback is especially critical when the experimental data samples are limited and some irregular experimental samples are presented, as illustrated in Fig. 3. As shown by the upper part of the figure, the light-red interval determined by the green (experimental) samples is the target of the interval updating. There are two irregular experimental samples highlighted in the blue box which are located far from the other green samples. If the general interval similarity is taken as the metric, one would get the updated samples and interval as shown by the lower part of Fig. 3. Although the range of the updated interval can be tuned towards the target interval, the inner location dispersions are clearly inconsistent, because the updated samples can only distribute uniformly along the interval.

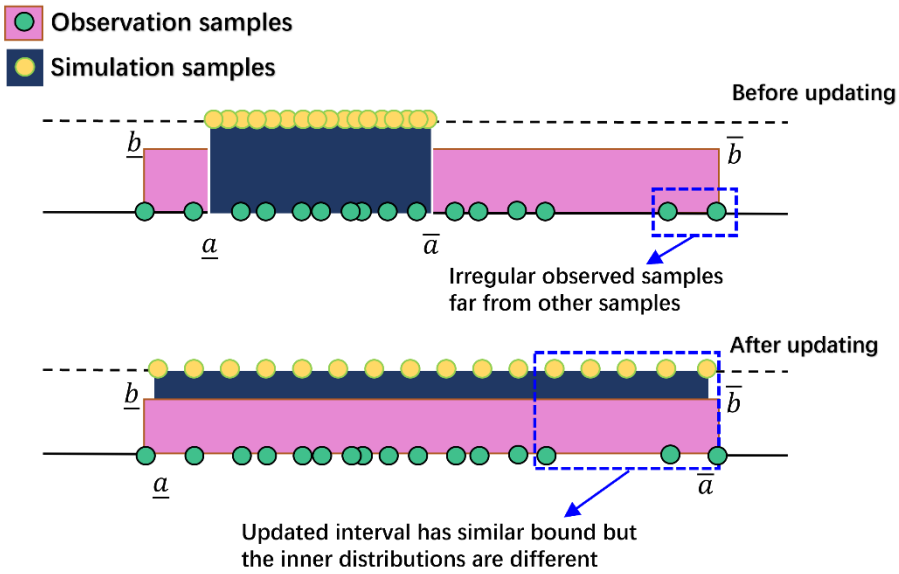

Fig. 3: Problem when only the interval range is considered in updating

It is consequently necessary to propose the so-called Sub-interval Similarity (SIS) metric to quantify the discrepancy between two intervals with the consideration of the location dispersion of the available samples. The principle of SIS is illustrated in Fig. 4, where the original experimental interval is divided into a certain number of sub-intervals. In this specific example, there are 16 experimental samples and 16 simulation samples. If the number of sub-intervals is determined as four, each sub-interval contains four samples. The bounds of each sub-interval are determined by the 1st and 4th samples of this sub-interval. The objective in model updating becomes to calibrate

each simulation sub-interval towards the experimental sub-interval.

The SIS metric is defined as follows

$$\mathrm{SIS}(A,B)|_{n_{sub}} = \frac{1}{n_{sub}} \sum_{j=1}^{n_{sub}} \{1 - \mathrm{ISF}(A^{(j)}, B^{(j)})\} \tag{10}$$

where n_{sub} is the number of the sub-intervals. The principle and method to determine n_{sub} are explained in the following Subsection 3.3. Because the updating process is executed on the sub-interval level, it is observed that the distribution property of the simulation samples in the lower part of Fig. 4 is similar to the one of the experimental samples, especially for Sub-interval #4, where the irregular experimental samples are presented.

The SIS metric and the Bhattacharyya distance [22] have the similar principle and objective to calibrate the distribution property. However, the Bhattacharyya distance requires elaborate data to estimate a precise PDF. In contrast, the SIS can make full use of the available experimental samples and hence achieve a balance between the benefit and cost.

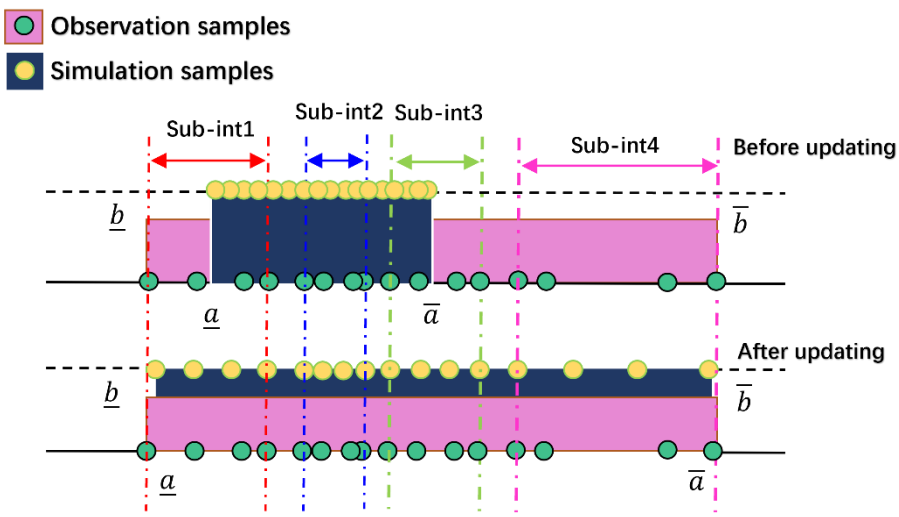

Fig. 4: Performance of the sub-interval similarity metric in updating

3.3 How to determine the number of sub-intervals

As shown in Eq. (10), the number of sub-intervals n_{sub} is the key parameter to calculate the SIS value. This subsection proposes an adaptive process to determine a suitable n_{sub} before the

execution of model updating. Some principles are prescribed as follows.

1) n_{sub} should be the same for both the experimental interval (termed as A) and the simulated interval (termed as B). The reason is indicated by Eq. (10) where the SIS is essentially the mean of the quantities relative to the Interval Similarity Function (ISF) of each subintervals in both intervals A and B. This requires the number of subintervals in A and B should be the same.

2) The whole interval is divided by specific samples, i.e. the data sample itself serves as the bound of the sub-interval, and one sample can belong to only one sub-interval. Note that, the whole interval will not be equally divided into n_{sub} parts. Inversely, the length of each sub-interval is different. The length of the sub-interval is determined by the position of the specific samples, e.g., as shown in Fig. 4.

3) Each sub-interval should contain a "nearly" average number of samples. For example, if an original interval with 16 samples is going to be divided into four sub-intervals, each of them should contain four samples, as shown in Fig. 4; if three sub-intervals are going to be divided from the 16 samples, the number of samples in Sub-interval #1-3 should be 5, 5, 6, respectively.

Following the above principles, the complete method and process for determining n_{sub} is listed as follows.

Step 1: Sort the experimental samples and the simulated simples following ascending order, respectively, and assign a series number to each sample from 1 to N_e (the number of experimental samples) or N_s (the number of simulated samples). In practical application, the number of experimental samples is generally less than the number of simulated samples, hence the following determination steps will take N_e as the reference.

Step 2: According to the principle prescribed above, determine the maximum number of sub-intervals as

$$n_{sub}^{(max)} = \left\lfloor \frac{N_e}{2} \right\rfloor \tag{11}$$

where $\lfloor \quad \rfloor$ is the round-down operator. When $n_{sub} = 1$, it is the extreme case that the

observed and simulated intervals are investigated as the original whole interval; when $n_{sub} = n_{sub}^{(max)}$, the intervals are divided with the highest resolution, leading each sub-interval to contain only two experimental samples, i.e. one sample defines the lower bound and the other defines the upper bound.

Step 3: The following key task is to find a suitable $n_{sub} \in \left[1, n_{sub}^{(max)}\right]$, which can balance the calculation cost and the ability to quantify the distribution property within the interval. This is achieved through a progressive decision process. Starting from $n_{sub} = 1$, progressively calculate the sub-interval similarity $\mathrm{SIS}(A,B)|_{n_{sub}=j}$. The progressive process is stopped, i.e. the suitable n_{sub} is found, when the following terminating criterion is satisfied:

$$n_{sub}^{(final)} = j, \forall \frac{\mathrm{abs}\left(\mathrm{SIS}(A,B)|_{n_{sub}=j} - \mathrm{SIS}(A,B)|_{n_{sub}=j-1}\right)}{\mathrm{SIS}(A,B)|_{n_{sub}=j}} < 1\%, \ j = 2, \dots, n_{sub}^{(max)} \tag{12}$$

After the number of sub-intervals is determined, it is also important to determine the bounds of the sub-intervals for a given n_{sub}. For the example with 20 experimental samples and 100 simulated samples, a detailed dividing configuration is shown in Table 1. The general treatment is to determine an average number of samples n_{av} in each sub-interval based on the number of sub-intervals n_{sub}:

$$n_{av} = round(\frac{N}{n_{sub}}) \tag{13}$$

where N is either N_e or N_s, representing the number of samples of the experimental data or the simulated data. As shown in Table 1, the treatment in Eq. (13) makes sure the number of samples in each sub-interval is "nearly" average, except the last few sub-intervals with flexible sample numbers to adjust the total number of samples in the original whole interval. As long as the number of samples is determined in each sub-interval, the bounds of the sub-interval are automatically determined by the position of the first and last sample points, as illustrated in Fig. 4.

Table 1: The sub-interval dividing configuration when $N_e = 20$ and $N_s = 100$

Sub-interval number	Experimental sub-intervals	simulated sub-intervals

1	20	100
2	10,10	50,50
3	7,7,6	33,33,34
4	5,5,5,5	25,25,25,25
5	4,4,4,4,4	20,20,20,20,20
6	3,3,3,3,4,4	17,17,17,17,17,15
7	3,3,3,3,3,3,2	14,14,14,14,14,15,15
8	2,2,2,2,3,3,3,3	13,13,13,13,13,13,13,9
9	2,2,2,2,2,2,3,3	11,11,11,11,11,11,11,11,12
10	2,2,2,2,2,2,2,2,2	10,10,10,10,10,10,10,10,10,10

An example of the progressive decision process with $N_e = 20$, $N_s = 100$, is illustrated in Fig. 5, where the intervals A and B have no overlap. It is observed that the curve of $\mathrm{SIS}(A,B)|_{n_{sub}}$ is monotonically increasing with the increase of n_{sub}. When $n_{sub} = 6$, the terminating criterion in Eq. (12) is satisfied, and the suitable number of sub-intervals is determined as 6.

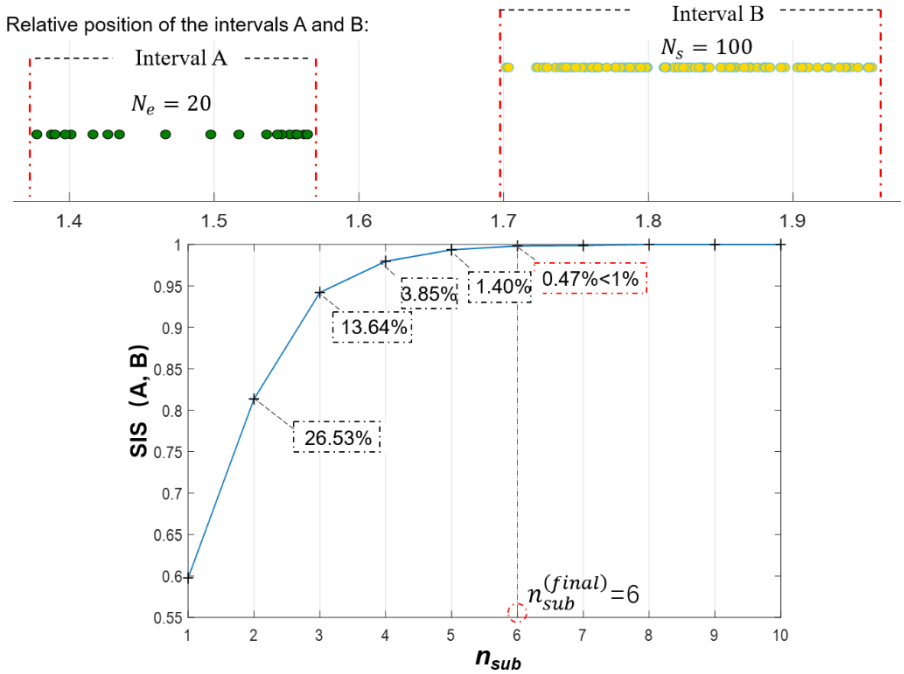

Fig. 5 Progressive decision process of the number of sub-intervals for two apart intervals

Besides the above complete determination process, an empirical equation is given as follows to make a fast estimation of n_{sub} in practical applications.

$$n_{sub} = \lceil 1.87(N_e - 1)^{2/5} \rceil \tag{14}$$

where $\lceil \ \ \rceil$ is the round-up operator. This equation only employs the number of experimental samples N_e, because the number of experimental samples is generally smaller than the number of simulated samples in practical applications. More explanation of the empirical equation can be found in Refs. [21,36].

4 Model updating with sub-interval similarity

This section focuses on how to integrate the above-defined SIS metric into the model updating framework. We will employ the SIS metric in both the stochastic model updating and the interval model updating, to demonstrate the generality of the SIS metric.

4.1 Stochastic model updating with approximate likelihood function

The stochastic updating in this paper specifically aims to calibrate the probabilistic distribution

of the input parameters, such that the distribution of the model outputs can represent the distribution features of the experimental samples. There is a wide range of methods for stochastic model updating, such as the sensitivity-based approach, optimization, and Bayesian approach. We select the Bayesian updating framework in this work and employ the MCMC algorithm for random sampling. For theoretic completeness, we simply recall the Bayesian approach as follows.

The foundation of Bayesian updating is the Bayes' theorem, expressed as

$$\mathrm{P}(\theta|\mathbf{Y}_e) = \frac{\mathrm{P}_L(\mathbf{Y}_e|\theta)\mathrm{P}(\theta)}{\mathrm{P}(\mathbf{Y}_e)}, \tag{14}$$

with its four components as the prior distribution of the calibrating coefficients $\mathrm{P}(\theta)$, the posterior distribution of the calibrating coefficients conditional to the existing experimental data $\mathrm{P}(\theta|\mathbf{Y}_e)$, the likelihood function $\mathrm{P}_L(\mathbf{Y}_e|\theta)$, and the evidence of the experimental data $\mathrm{P}(\mathbf{Y}_e)$. Detailed information of the four components of Bayes' theorem is omitted, while the fundamental work Ref. [9] is suggested in case more background information is required. Please note, the calibrating coefficients θ is not the model input parameters $\mathbf{X}$, but their distribution coefficients, e.g. means or variances. Because the objective of stochastic model updating is no longer to calibrate the input parameters themselves, but their distribution properties.

A key development of the Bayes' theorem focuses on the likelihood function $\mathrm{P}_L(\mathbf{Y}_e|\theta)$, which needs to be customized to adapt to different updating objectives. The likelihood function is originally defined as the distribution of the experiment observations conditional to the calibrating coefficients. It essentially acts as the connection between the existing observation data and the coefficient to be calibrated. Ref. [22] proposes an approximate version of the likelihood function, with high efficiency and direct connection with the discrepancy between experimental observation and the model simulation, expressed as

$$P_L(\mathbf{Y}_e|\mathbf{X}) = \frac{1}{\sigma\sqrt{2\pi}}\exp\left\{-\frac{\mathrm{SIS}(\mathbf{Y}_e,\mathbf{Y}_S(\theta))^2}{2\sigma^2}\right\}. \tag{15}$$

It is observed that the approximate likelihood function directly integrates the SIS metric, such that the calibrating coefficient θ can be updated ensuring SIS takes the minimum value while the

likelihood takes the maximum probability. The MCMC algorithm is employed to execute the iterative process to generate samples from the posterior distribution of θ. The MCMC algorithm is based on the adaptive Metropolis-Hastings method to accept instances of θ resulting higher value of the likelihood function. Detailed information of the widely-applied method is omitted, while more information can be found from the original paper Ref. [11] and the tutorial paper Ref. [14].

4.2 Interval updating with customized objective function

Different from the stochastic model updating, the interval updating is performed with no hypothesis of probabilistic distributions. Both the parameters and model outputs are described as intervals, and hence the objective is to calibrate the parameter midpoint $E(\mathrm{x})$ and interval length $L(\mathrm{x})$ of the interval $[\overline{\mathrm{x}}, \underline{\mathrm{x}}]$, such that the interval of the model outputs is coincident with the experimental data. The interval updating can be therefore formulated as an optimization problem, where the SIS metric is served directly as the objective function and the midpoint and length of the parameter interval are the design parameters. The optimization is expressed as:

$$\begin{gathered} \textit{Find } \hat{E}(\mathrm{x}) \textit{ and } \hat{L}(\mathrm{x}), \\ \textit{Minimizing } f_{obj}(E(\mathrm{x}), L(\mathrm{x})) = \mathrm{SIS}(\mathbf{Y}_e, \mathbf{Y}_s(E, L)), \\ \textit{Subject to } \begin{cases} E(\mathrm{x}) \in [\overline{\mathrm{x}}, \underline{\mathrm{x}}] \\ L(\mathrm{x}) \in \left[0, \frac{\overline{\mathrm{x}} - \underline{\mathrm{x}}}{2}\right] \end{cases}, \end{gathered} \tag{16}$$

where $[\overline{\mathrm{x}}, \underline{\mathrm{x}}]$ is the pre-determined largest range of the model parameters. This range is determined based on the prior knowledge of the investigated problem, such as the allowed range of the geometric parameters or the possible material parameters with physical meaning.

Although the constraint in Eq. (16) is simply linear, the optimization problem is intractable because of the complex and nonlinear relationship between the objective function and the parameter interval midpoint $E(\mathrm{x})$ and length $L(\mathrm{x})$. The overall optimization problem essentially consists of a double-loop framework, where the inner loop is dedicated to calculating the objective function from the parameter interval properties, based on random sampling and SIS calculation; while the outer loop focuses on searching the $\hat{E}(\mathrm{x})$ and $\hat{L}(\mathrm{x})$ to get the minimal objective function. A

complete flowchart of interval model updating including the double-loop optimization and the detailed steps of SIS metric calculation is illustrated in Fig. 6.

Starting from a pre-determined range of parameters $\left[\overline{\mathbf{x}_0}, \underline{\mathbf{x}_0}\right]$, which represents the gross knowledge from engineering judgment, the initial midpoint $E_0(\mathbf{x})$ and length $L_0(\mathbf{x})$ of the interval are available. The inner loop of SIS calculation is performed first based on $E_0(\mathbf{x})$ and $L_0(\mathbf{x})$ to generate N_s simulated parameter samples $\mathbf{X}_s$, which uniformly distribute along the pre-determined interval. The system model $f(\mathbf{X}_s)$ is then executed N_s times to generate the simulated model output $\mathbf{Y}_s$. Please note the treatment of generating the samples uniformly does not necessarily admits that the parameters follow uniform distribution within the interval. It is simply a practical and efficient tool to estimate the possible output space based on random sampling process. It is possible to assess different auxiliary distributions, e.g. uniform, Gaussian, and Beta distributions, in the inner loop. When the number of samples is large enough, the influence of different distributions is limited, as it can be demonstrated in the example section. Another work resorting the Monte Carlo sampling for interval propagation is the multilevel quasi-Monte Carlo approach [33] based on the Cauchy random variables.

Jump out from the inner loop with $\mathbf{Y}_s$, and together with the experimental data $\mathbf{Y}_e$, the next step is to calculate the Subset Interval Similarity (SIS) metric. This task is divided into several sub-steps, in which the first is the determination of the number of sub-intervals n_{sub} following the procedure in Sec. 3.3 and Eq. (12). For each sub-interval, the Relative Position Operator (RPO) between the simulated one and the experimental one is determined following Eq. (7). Afterwards the Interval Similarity Function (ISF) of each sub-interval is calculated following Eq. (9). Finally, the integrated SIS metric considering all sub-intervals is determined following Eq. (10).

Till now the objective function, i.e. the SIS metric, is calculated for the instance of $E(\mathrm{x})$ and $L(\mathrm{x})$. And now it comes to the outer loop of optimization. Various optimization tools can be selected in this step, such as the classical gradient-based algorithm, the biomimetic algorithm, and the intelligent deep learning algorithms, depending on the complexity of the problem. Being outside of

the scope of this work, the comparison of different optimization algorithms is omitted in this paper. We select the Particle Swarm Optimization (PSO) in this work, because of its advantages as to be applicable for large searching space, and to be robust for strong nonlinearity of objective functions. The convergence condition of PSO is that the change of the fitness value is less than a threshold value or the number of iterations reaches the pre-determined limit. After the convergence of PSO, the minimized SIS metric, as well as the optimized interval properties of the parameters $E(\mathbf{x})$ and $L(\mathbf{x})$ is obtained.

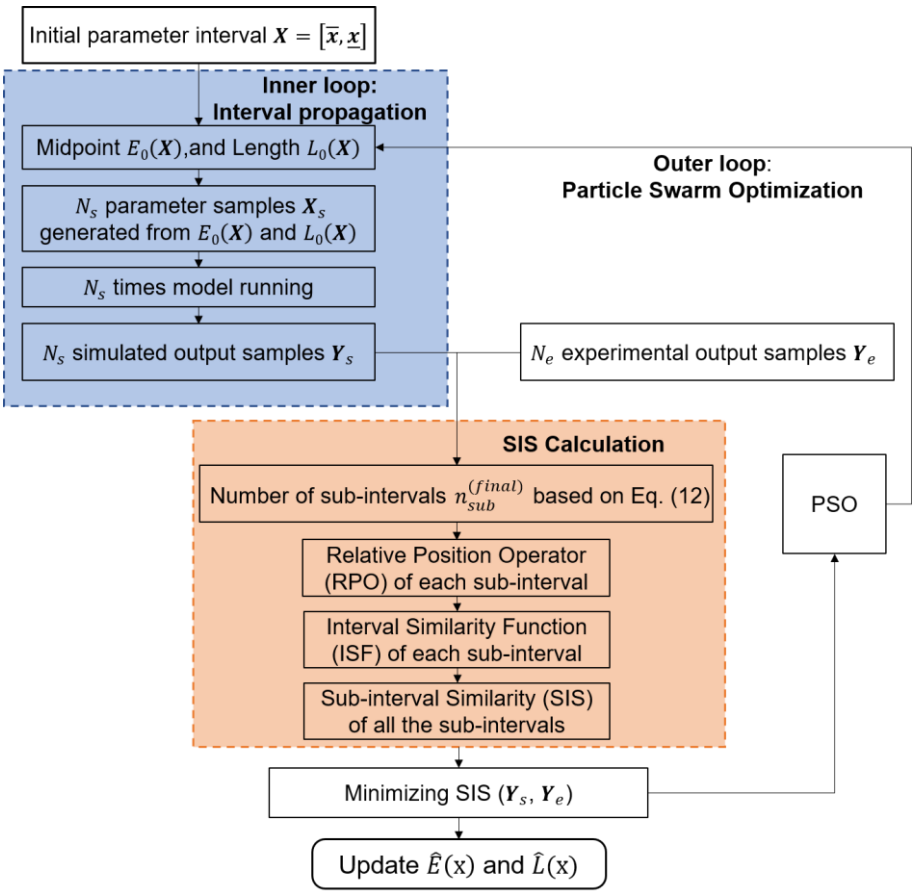

Fig. 6 Flowchart of the double-loop interval updating and SIS calculation

5 Case studies

5.1 The 3-dof mass-spring example

The performance of the SIS metric in both stochastic and interval model updating is

demonstrated in the classical three-dof mass-spring example, first proposed by Mottershead et al. [5], as illustrated in Fig. 7. In the following stochastic updating and interval updating, different parameter configurations originated from Refs. [22] and [34] are adopted, such that the updating results in this work will be compared with different published works in the following two subsections, respectively. It is necessary to mention that, although in this example we select a low number of parameters, in a practical updating problem, it is common to encounter a much larger number of parameters than the output features [37]. This will lead to an ill-posed optimization problem with non-unique solutions of the updating process. A common treatment for this issue is the sensitivity analysis prior to the updating process to identify the significant parameters which are really necessary to be updated in the following process.

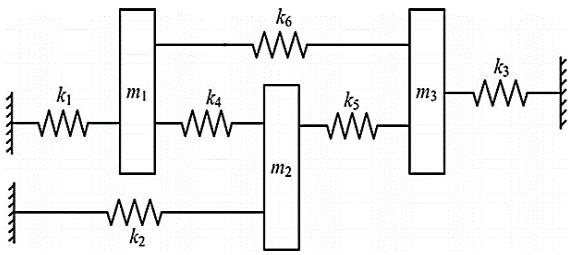

Fig. 7 The simulated three-dof mass-spring system

5.1.1 Stochastic updating using Bayesian MCMC

The parameter configuration in this subsection includes deterministic parameters of the mass m_1=0.7kg, m_2=0.5kg, m_3=0.3kg and spring stiffness k_4=k_5=k_6=5.0N/m. The remaining spring stiffness coefficients k_1, k_2, k_3 are assumed to be random variables following Gaussian distribution with the undetermined means μ_1, μ, μ_3 and standard deviations σ_1, σ_2, σ_3, which will be updated in this example. The three natural frequencies f_1, f_2, f_3 are taken as the model outputs. The "experimental" output data (i.e., the updating target) is simulated by assigning a set of target values to the parameter means and standard deviations, as shown in Table 2, and generating N_e=100 samples of k_1- k_3 and subsequently obtaining 100 samples of f_1- f_3. The initial values of the mean and standard deviation are selected on purpose to be different from the target values, such that the updating effect can be assessed by comparing the frequencies before and after updating.

Table 2: The target and initial uncertainty properties of k_1- k_3

Parameter	Uncertainty characteristic	Target value	Initial value
k_1	Gaussian, $\mu_1 \in [3,7], \sigma_1 \in [0,0.5]$	$\mu_1 = 4, \sigma_1 = 0.3$	$\mu_1 = 3, \sigma_1 = 0.1$
k_2	Gaussian, $\mu_2 \in [3,7], \sigma_2 \in [0,0.5]$	$\mu_2 = 5, \sigma_2 = 0.1$	$\mu_2 = 4, \sigma_2 = 0.2$
k_3	Gaussian, $\mu_3 \in [3,7], \sigma_3 \in [0,0.5]$	$\mu_3 = 6, \sigma_3 = 0.2$	$\mu_3 = 5, \sigma_3 = 0.3$

A) Comparison of the means and standard derivations of the input parameters

The prior distributions of the means and standard deviations are adopted as uniform distributions along with the pre-determined ranges as shown in Table 2. The MCMC algorithm is employed to iteratively generate samples and such that to estimate the posterior distributions. The number of samples in each MCMC iteration is set to be 1000. Consequently, the simulated intervals of f_1- f_3 with 1000 samples and the experimental intervals with 100 samples are utilized to calculate the SIS metric, which is subsequently utilized to construct the likelihood function following Eq. (15). In this example, after 13 iterations the MCMC algorithm converges, and the posterior 1000 samples of the means and standard deviations are obtained. Scatters and histograms of these 1000 samples are illustrated in Fig. 8. The diagonal elements present the histograms which can be used to estimate the posterior distributions of the means μ_{1-3} and standard deviations σ_{1-3}. It is shown the posterior distributions are significantly changed from the prior ones, which are no longer uniformly distributed along the interval, but sharply centralized to a middle value. This value is regarded as the "updated value" obtained by estimating the means of the 1000 samples and listed in Table 3.

The relative errors of the initial and updated means and standard deviations are compared with the target one as illustrated in Fig. 9. It is shown the relative errors of the updated values are significantly reduced compared with the initial ones, implying the feasibility of the stochastic model updating algorithm and the SIS metrics. The updating results in Ref. [22], derived from the same

parameter configuration, is also presented in Table 3 and Fig. 9 for comparison. It can be seen that the updated values using the proposed approach are similar to the ones from Ref. [22], and the relative errors are also comparable.

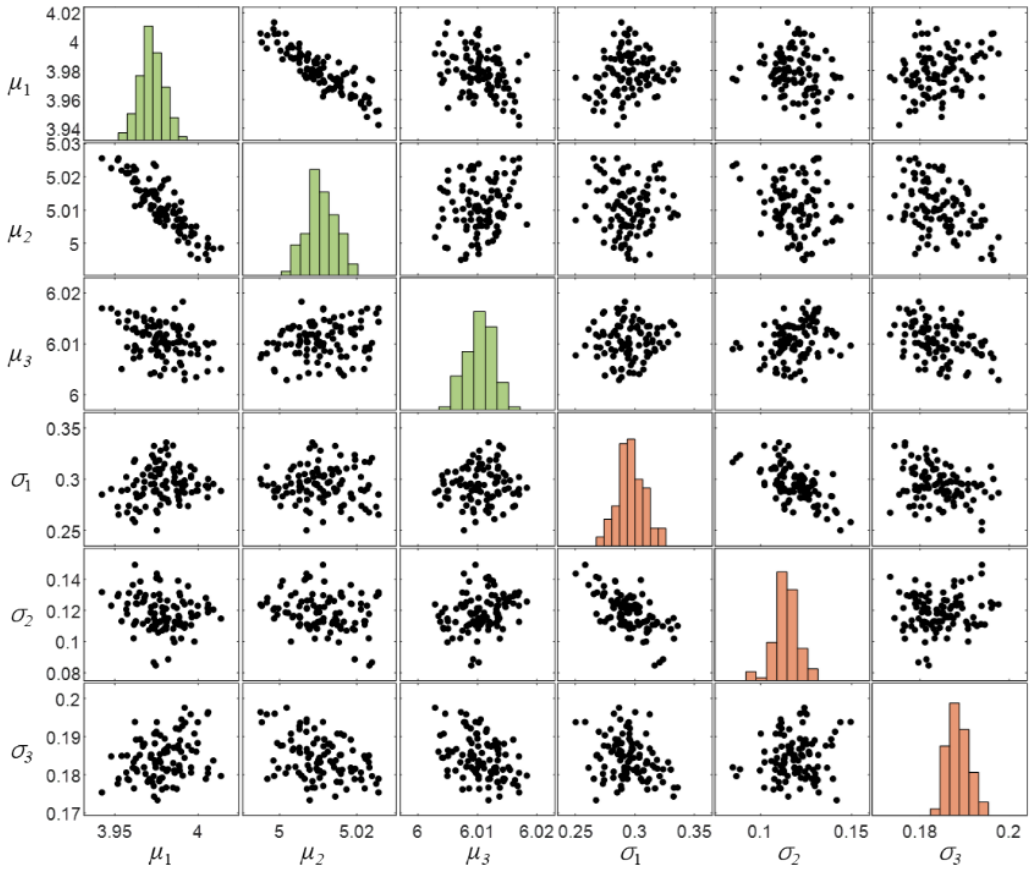

Fig. 8 The scatters and histograms of the posterior samples of the means μ_{1-3} and standard deviations σ_{1-3}

Table 3: Error comparison of updated means and standard deviations of k_1-k_3

	Target value	Initial value	Updated value	Result in Ref. [22]
μ_1	4	3	3.9788	4.0386
μ_2	5	4	5.0108	5.0102
μ_3	6	5	6.0106	6.0253
σ_1	0.3	0.1	0.2950	0.3067

σ_2	0.1	0.2	0.1098	0.0937
σ_3	0.2	0.3	0.1844	0.1843

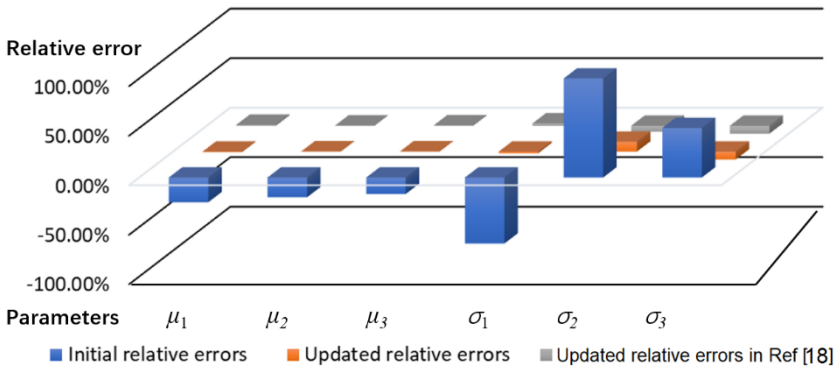

Fig. 9 The relative errors of the calibrating values μ_{1-3} and σ_{1-3}

A further investigation is focused on the actual distribution of the parameters k_1- k_3 based on the above-updated means μ_{1-3} and standard derivations σ_{1-3}. The Gaussian PDFs of the target, initial, and updated parameters are illustrated in Fig. 10. It is obvious that the initial PDFs differ from the target PDFs in not only the positions (controlled by the means) but also the dispersion degree (controlled by the standard derivations). After the updating procedure, the updated PDFs are well consistent with the target ones.

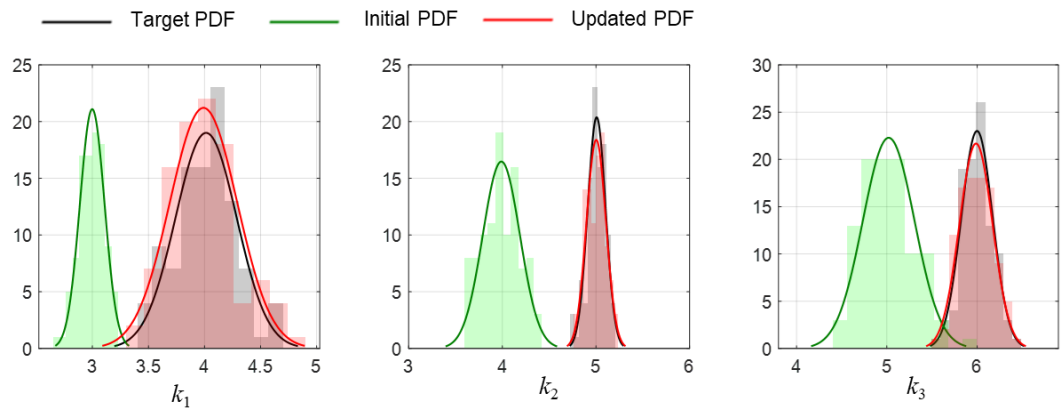

Fig. 10 Target, initial, and updated PDFs of k_1, k_2, k_3

B) Comparison of the model outputs with SIS metrics

In this example, the number of experimental samples N_e is 100, the number of simulated

samples N_s in each iteration is 1000. Following Eq. (12), the number of sub-intervals is determined as $n_{sub} = 20$. Consequently, the sample number in each sub-interval for experimental data and simulated data is 5 and 50, respectively. Since the samples are sorted in ascending order, as long as the sample numbers are determined in sub-intervals, the bounds of the sub-intervals are determined, as illustrated in Fig. 11. When considering all samples together as a whole interval, the upper and lower boundaries of outputs f_1- f_3 become close to the target bounds after model updating. More than that, the bounds of each updated sub-interval are also close to that of the target sub-interval, even though each updated sub-interval contains 50 samples while the target one contains 5 experimental samples. This result shows that the proposed non-probabilistic uncertainty metric, SIS, is able to measure the distribution similarity between two datasets, with the superiority of avoiding the complicated calculation to find the approximation of the probability distribution.

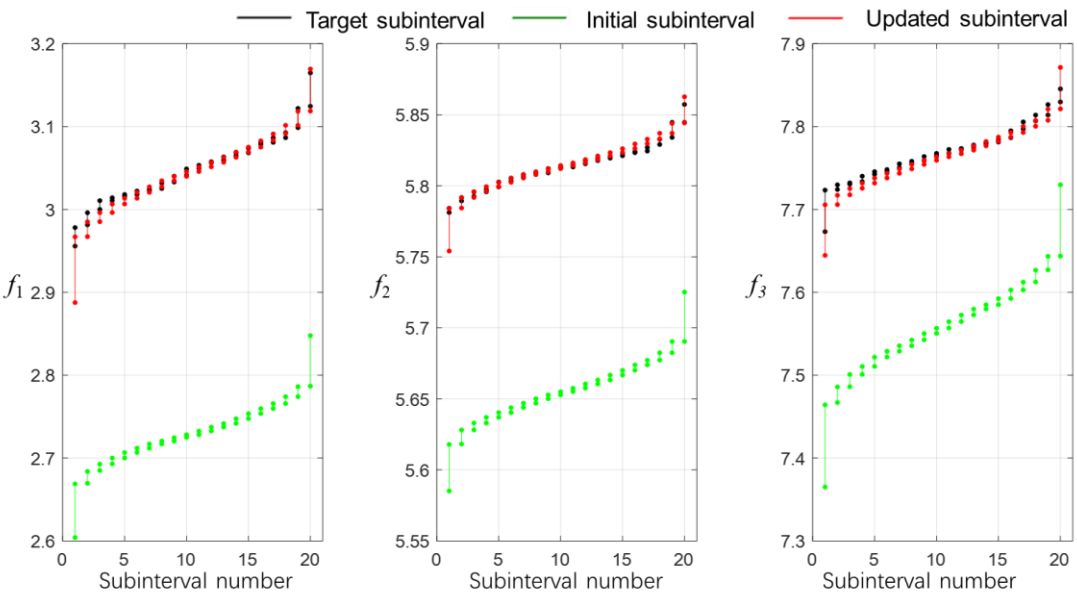

Fig. 11 Target, initial and updated sub-interval bounds of outputs f_1- f_3

For the comparison of calculation cost between the proposed SIS metric and the Bhattacharyya distance in Ref. [22], we focus on the dimensions of the model output feature. The SIS approximates the similarity between two datasets based on the simple interval arithmetic operations, leading it to be not highly sensitive to the dimension of the quantity of interest. While the evaluation of the Bhattacharyya distance is based on the overlap between two joint-PDFs, which is clearly influenced

by the quantity dimensions.

Herein an example consisting of two datasets is given to explain the advantages of SIS in calculation efficiency. Randomly generate two datasets with 1000 samples, namely Data #1 and Data #2. Consider different cases when the datasets are presented in different numbers of dimensions, the time to calculate the corresponding Bhattacharyya distance and the SIS metric are shown in Table 4 and illustrated in Fig. 12.

Table 4 Calculation time* of the Bhattacharyya distance (BD) and the SIS metric

Dimensions		1	3	6	7	8	9
Calculation Time / s	BD	0.00163	0.00259	0.0134	0.208	4.365	1280.80
	SIS	0.00068	0.00091	0.00112	0.00146	0.00155	0.002032

* executed on a consumer-laptop with the Intel(R) Core (TM) i7 CPU

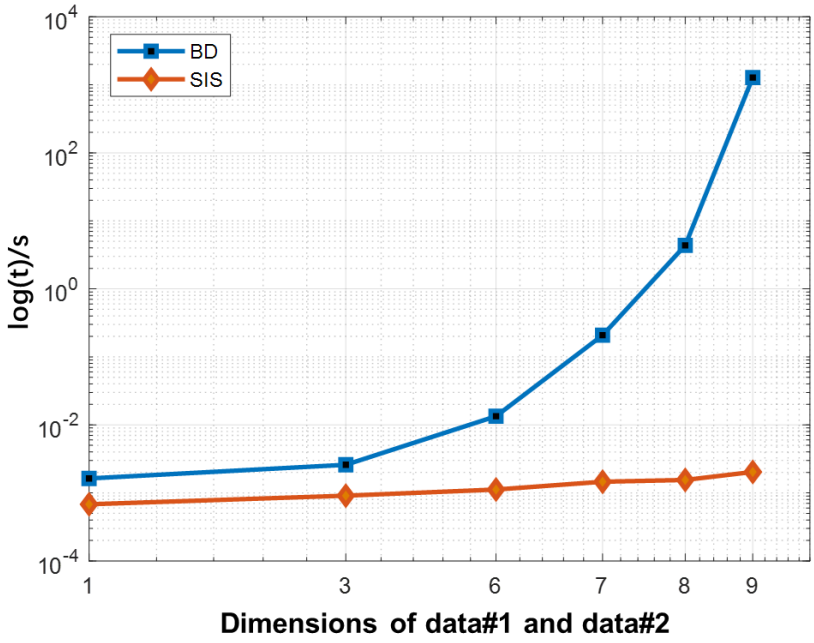

Fig. 12 Comparison of calculation time between the Bhattacharyya distance and SIS with increasing data dimensions

As shown in Fig. 12, when the dimension of the datasets is low, the calculations of the

Bhattacharyya distance and the SIS are both fast and the time consumption is comparable. However, with the increase of the dimension, the calculation time of the Bhattacharyya distance increases dramatically while the calculation of the SIS remains very fast. For example, when the dimension is 9, the calculation time of the Bhattacharyya distance is 1280.80s, which is about 492 times higher than that of the SIS. Note that, in the process of stochastic model updating, the calibrating metric will be called hundreds of thousands of times, leading the Bhattacharyya distance to be prohibitive for high dimensional applications. While the SIS metric is less sensitive to the dimension of the investigating problem.

However, it is necessary to mention that, although the calculation of the Bhattacharyya distance is sensitive to the data dimension, it possesses the superiority that it can capture the correlation among multi-dimensions. The SIS deals with the multidimensional data in a much simplifized manner that to first marginalize the samples to each dimension, and then calculate the mean of the SIS on all the dimensions. This dramatically reduces the calculation time, but as a limitation, it ignores the correlation features of the multidimensional data.

5.1.2 Interval updating using optimization with the SIS metric

This sub-section employs the same 3-dof mass-spring system, however, with a different parameter configuration from Sec. 5.1.1. The current parameter configuration is proposed to be the same as the one used in Ref. [31], such that the updating result can be assessed by the comparison with the ones in the reference. Here k_1, k_2, and k_5 are assumed as interval variables, while the remaining parameters are set to be constants, i.e. $m_1 = m_2 = m_3 = 1$kg, $k_3 = k_4 = 1$N/m, and $k_6 = 3$N/m. The natural frequencies f_1, f_2, and f_3, and the norm value of the eigenvectors $|\varphi(1, 1)|$ are taken as output features.

From Ref. [31], the midpoints of the interval variables k_1, k_2, and k_5 are all set to be the same value 1, hence only the length are the quantity to be updated in this example. Following the same principle to set the target values of the updating process, the "target length" of the interval variables k_1, k_2, and k_5 are assigned as 0.4, as shown in Table 5. In other words, k_1, k_2, and k_5

have the same target intervals as [0.8, 1.2]. The initial value of the length is set to be 1.0. As shown in Table 5, there are two sets of updated results, one of which is obtained based on 10000 experimental samples, while another is based on 100 samples. These "experimental target" samples are generated by first generating 10000 (or 100) samples of k_1, k_2, and k_5 generated within their initial intervals and subsequently running the model 10000 (or 100) times to calculate the output feature samples. This treatment of employing different numbers of target samples in this example is aimed at assessing whether the SIS metric has a feasible performance with limited experimental data.

A) Comparison of the intervals of the input parameters

The PSO algorithm is employed to minimize the SIS between the simulated interval and the target interval of the output features. The target, initial, and updated interval lengths of k_1, k_2, and k_5 are listed in Table 5. It is observed that the updated results based on 100 and 10000 target samples are similar, and both of them are close to the target value. This, on the one hand, demonstrates the feasibility of the SIS metric in the interval updating framework, and on the other hand, demonstrates the proposed SIS metric is feasible for limited target (or experimental) data.

Table 5 The target, initial, and updated lengths of k_1, k_2, and k_5

Interval parameters	Target	Initial	Updated (N_e =100)	Updated (N_e =10000)
k_1	0.4	1.0	0.4058	0.3970
k_2	0.4	1.0	0.4002	0.4024
k_5	0.4	1.0	0.4062	0.4024

Table 6 presents the relative errors of the lower and upper bounds of the initial and updated intervals regarding the target intervals. It is observed that the updated errors are dramatically reduced from the initial errors. The bounds errors updated based on 10000 target samples and the ones based on 100 samples are similar. Taking the same parameter configuration, the updated results by Ref. [31] is presented in Table 6. It is interesting to compare that the updated errors in Ref [31] with 10000 target samples are similar to the error in the current work with only 100 target samples,

demonstrating the efficiency of the proposed SIS metric in interval updating.

Table 6 Initial and updated relative errors of interval bounds of k_1, k_2, and k_5

Parameters	Initial error %	Updated error % (N_e=100)	Updated error % (N_e=10000)	Updated error % in Ref. [31] (N_e=10000)
k_1	[-37.5 25.0]	[-0.36, 0.24]	[0.19, -0.12]	[0.1, -0.2]
k_2	[-37.5 25.0]	[-0.01, 0.01]	[-0.15, 0.10]	[0.5, 0.0]
k_5	[-37.5 25.0]	[-0.39, 0.26]	[-0.26, 0.17]	[0.3, -0.1]

B) Comparison of the intervals of the model outputs

The three natural frequencies and the norm of the eigenvector at the first degree of freedom are predicted based on the updated intervals of the input parameters. Ref. [31] employs the treatment to randomly generate 10000 samples of the input paramters and propagate through the model to estimate the space of the output intervals. We take the same treatment starting from the true interval of k_1, k_2, and k_5, [0.8, 1.2], after 10000 model evalution, obtaining the target intervals of the output feature, as shown in Table 7. The updated intervals of the outputs are presented in the table using different sampling distributions in the inner loop (recall Fig. 6). It is demonstrated that, on the one hand, the updated output intervals have a high precision compared with the target intervals; on the other hand, the updated intervals based on different sampling distributions are similar, implying the selection of different auxiliary distribution, acting as interval propagation tools, have limited influence of the updating results.

Table 7 Intervals of the updated outputs employing different auxiliary distribution with the parameter intervals

Employed distributions	f_1	f_2	f_3	$\|\varphi(1, 1)\|$	Mean relative error
Uniform	[0.8666, 1.1294]	[3.5477, 4.4441]	[7.8054, 8.2027]	[0.5491, 0.6041]	[0.42%, 0.08%]
Gaussian	[0.8891, 1.106]	[3.6005, 4.3487]	[7.8358, 8.186]	[0.5514,0.5984]	[0.83%, 1.26%]

Beta	[0.8776.1.1154]	[3.6395, 4.3532]	[7.9627, 8.177]	[0.5597, 0.5915]	[1.56%, 1.34%]
Target interval	[0.8693, 1.1279]	[3.5915, 4.4421]	[7.8114, 8.1978]	[0.5487, 0.6035]	

Fig. 13 illustrates the interval bound squares of the output features in the plane of f_1 vs. f_2, and the plane of f_3 vs. $|\varphi(1, 1)|$. Since the midpoint of the intervals of input parameters k_1, k_2, and k_5 are all assigned to be 1.0, the midpoints of the obtained output features are coinciding among the target, initial, and updated squares. However, the outlines of the squares have been clearly calibrated as the updated squares are nearly coincident with the target square. The updated samples and squares in Fig. 13 are obtained based on 100 target samples, once again demonstrating the interval updating with SIS metric is feasible for a limited number of the experimental samples.

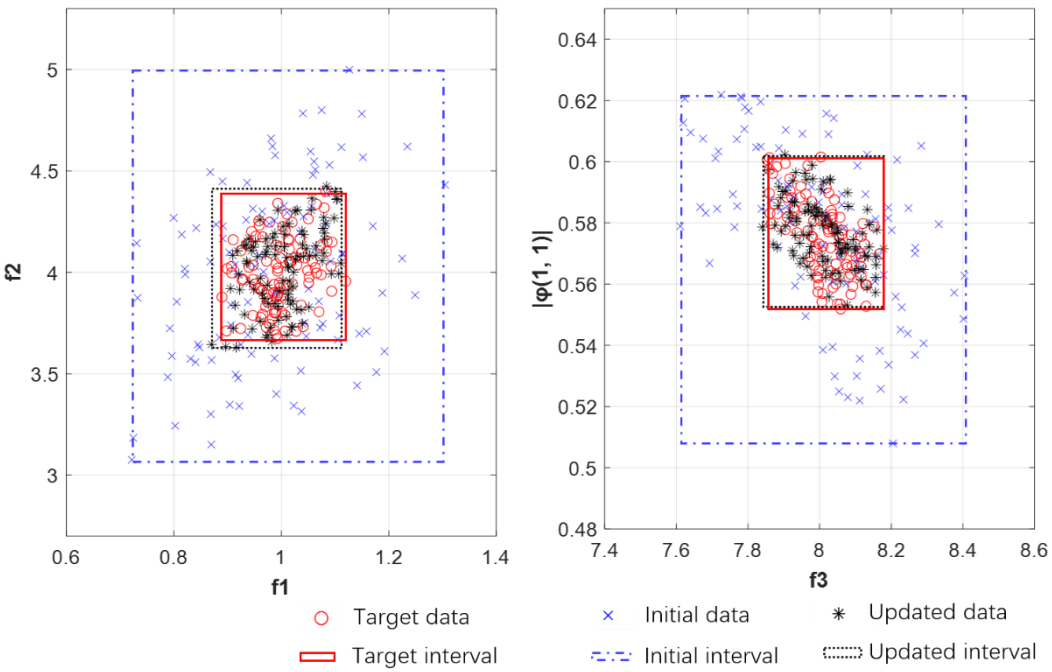

Fig. 13 Boundary square of the target, initial, and updated features

5.2 The practical steel plates example

This subsection employs the example with 55 identical steel plates, which were first tested by Fang et al. [32]. The 55 plates are designed in the same geometry property, 600 mm (length) ×120 mm (width) × 3 mm (thickness), with the same material property, i.e. Young's modulus $E = 210$ GPa, shear modulus $G = 83$ GPa, and density $\rho = 7860$ Kg/m^3. However, because of the

uncertainties sourced from manufacturing tolerance, material heterogeneity, and test randomness, the tested natural frequencies on the 55 plates exhibit considerable dispersity. The intervals of the tested five order natural frequencies are listed in Table 8. A second-order response surface model of the finite element model of the plates was built by Deng et al. [34], expressed as

$$\begin{aligned} f_1 &= 1.31 + 0.2152E - 0.01455G - 0.0002813E^2 - 0.0004878E \cdot G + 0.0006576G^2 \\ f_2 &= 44.08 + 0.5145E - 0.1333G + 0.0002943E^2 - 0.004055E \cdot G + 0.005588G^2 \\ f_3 &= 52.85 - 0.1156E + 1.455G + 0.0006092E^2 + 0.0002019E \cdot G - 0.005634G^2 \\ f_4 &= 375.4 - 3.207E - 0.4291G + 0.02202E^2 - 0.009699E \cdot G + 0.01383G^2 \\ f_5 &= 79.55 + 0.255E + 2.804G - 0.0005059E^2 - 0.001249E \cdot G - 0.009833G^2 \end{aligned} . \quad (17)$$

Based on the surrogate model, the intervals of the natural frequencies are predicted and listed in Table 8. By the comparison of the two sets of intervals, the relative errors are quite low, implying the predicted intervals can represent the property of the tested data. The reason to introduce the predicted intervals in Ref. [34] is that Fang et al. [32] only presented the bounds of the frequency intervals but not the detailed 55 test samples. Only the bounds are not enough to evaluate the SIS metric. Consequently, we propose to utilize the surrogate model and the predicted intervals, which can still represent the features of the practical test data.

This example employs Young's modulus E and shear modulus G as the input parameters to be calibrated, and the first five order natural frequencies as output features. Ref. [34] has predicted the input intervals $E \in [196.2, 204.8]$, $G \in [79.1, 83.7]$, which can reproduce the frequency intervals in Table 8. The input intervals are hence adopted as the target intervals in the following updating process. 55 samples of E and G are randomly generated from the intervals and propagated through the model to the frequencies, generating 55 natural frequency samples, which are adopted as the target output features.

The relative position of the real experiment interval and the target intervals and samples are illustrated as 3-dimensional interval cubes in the space of $f_{1\text{-}3}$, and $f_{3\text{-}5}$, as shown in Fig. 14. It is observed that the simulated cubes defined by the 55 simulated samples are coincident with the practically measured cubes, implying it is reasonable to take simulated intervals and samples as the

target in the following evaluation process of the SIS metric.

Table 8 Intervals of the tested natural frequencies

Frequency	f_1	f_2	f_3	f_4	f_5
Intervals in Ref. [32]	[42.66,43.64]	[118.29,121.03]	[133.24,136.54]	[234.07,239.20]	[274.29,280.64]
Intervals in Ref. [34]	[42.81,43.81]	[118.28,121.38]	[133.25,137.05]	[232.25,239.10]	[272.77,280.36]
Relative error	[0.35%.0.39%]	[-0.01%,0.29%]	[0.01%,0.37%]	[-0.78%,-0.04%]	[-0.55%, -0.10%]

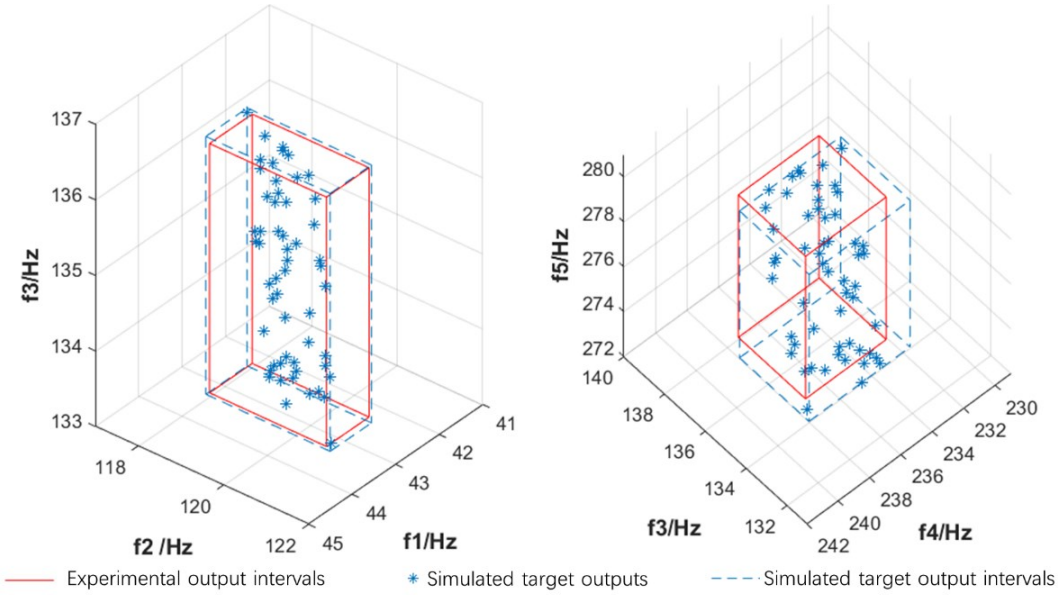

Fig. 14 Cubes and samples of the simulated target data and the measured data

The PSO algorithm is employed to minimize the SIS metric value in the optimization problem. The number of simulated samples is set to be 10000 in each iteration, implying the SIS metric is calculated between the simulated interval with $N_s = 10000$, and the target interval with $N_e = 55$. The updated bounds of the input intervals are presented in Table 9. The relative errors of the updated bound regarding the target values are quite small, demonstrating the effect of the SIS metric in the

interval updating problem.

Table 9 The target and updated bounds of the parameter intervals

Parameters	Target intervals	Updated intervals	Relative errors
E (GPa)	[196.2, 204.8]	[196.59,204.61]	[0.20%, -0.09%]
G (GPa)	[79.1, 83.7]	[79.21, 83.91]	[0.14%, 0.25%]

More attention to this example is placed on how the different numbers of sub-intervals will influence the evaluation of SIS metrics and subsequently influence the updating outcomes. According to Eq. (12), the optimal number of sub-intervals is 8. The updated parameter bounds and the mean of their relative errors with different numbers of sub-intervals are illustrated in Fig. 15 and Fig. 16. When the number of sub-intervals $n_{sub} = 1$, i.e. only the outer bounds of the interval are considered, the errors of the parameter interval are obviously higher than the other cases. However, with the increase of the subinterval numbers, the updated accuracies improved rapidly and convey finally. This demonstrates merely considering the outer bounds is not enough for interval updating in the presence of limited experimental data, i.e. 55 samples in this example. The subinterval can quantify more uncertain information of the distribution of experimental data.

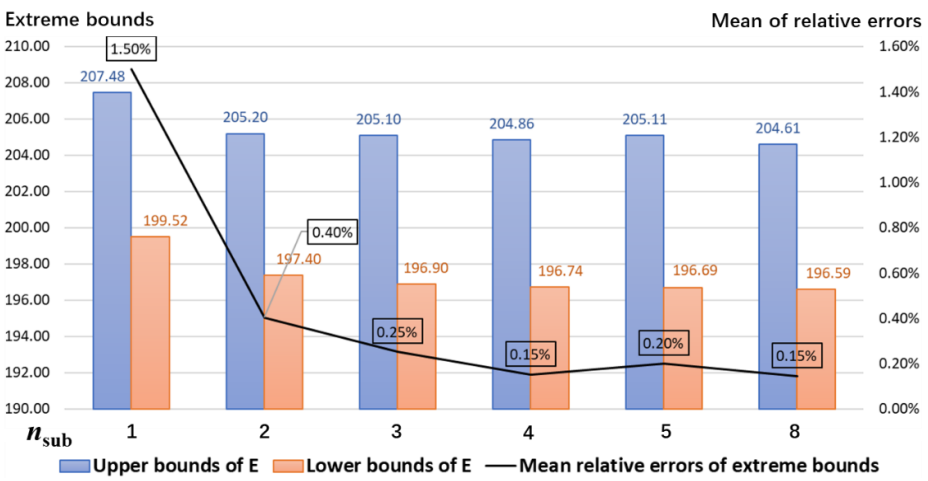

Fig. 15 The relative errors of updated bounds of E with increase numbers of sub-intervals

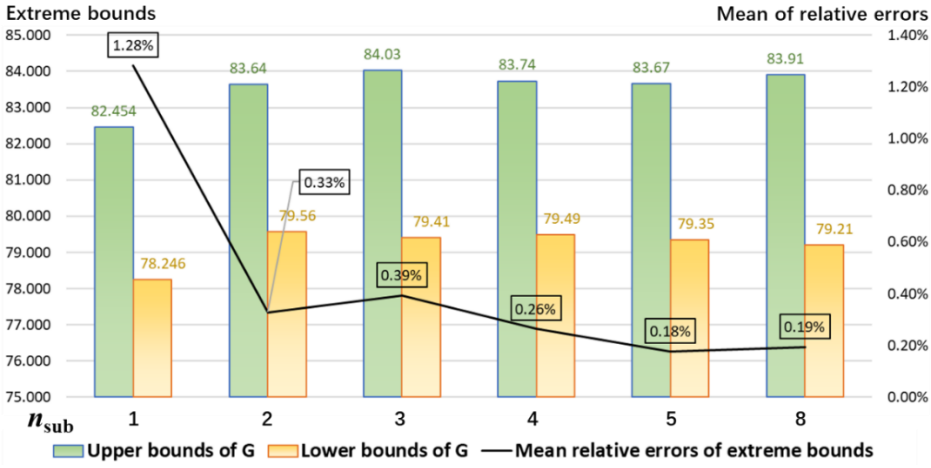

Fig. 16 The relative errors of updated bounds of G with increased numbers of sub-intervals

The relative position of the target and updated output features are illustrated as the three-dimensional cubes in the space of the natural frequencies, as shown in Fig. 17. This figure gives the comparison between the results with n_{sub}=1 and n_{sub}=8. Clearly, when n_{sub}=1 the SIS metric degrades into the normal interval similarity. Because the internal samples location feature is not considered, the updated result is apart from the target. Once dividing the datasets into several sub-datasets, the SIS metric is more accurate to describe the uncertainties between the target outputs and the simulated outputs, which significantly improves the accuracy of the interval model updating outcome.

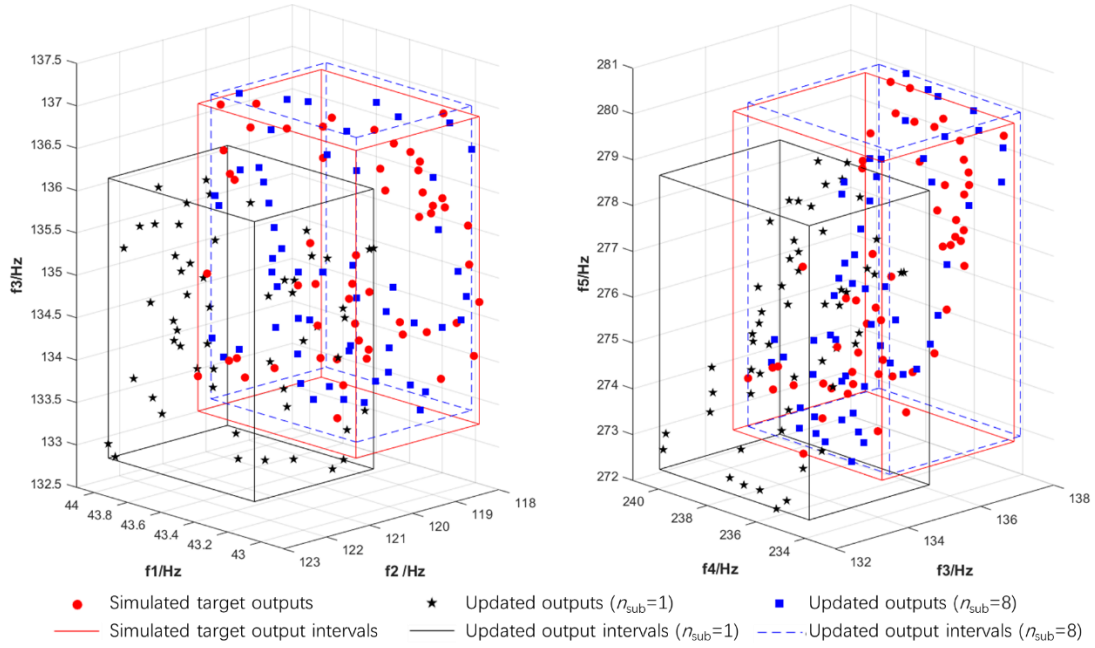

Fig. 17 Target and updated natural frequencies with sub-interval numbers n_{sub}=1 and n_{sub}=16

6 Conclusion and perspectives

The Sub-interval Similarity (SIS) is proposed as a general-purpose UQ metric with the universality to be feasible in both stochastic model updating and interval model updating. In stochastic updating where the investigating parameters are assumed to follow probabilistic distributions, the SIS is proven to be capable of calibrating the distribution properties, e.g. mean and variance, of the parameters. In the interval updating, the SIS is demonstrated to be feasible in calibrating the midpoint and length of the parameter intervals.

The SIS metric is motivated by the classical interval similarity function, but it possesses the superiority that it is capable of quantifying the randomness of the sample location dispersion, especially when the available experimental samples are limited. From this point of view, the SIS metric is similar to the Bhattacharyya distance to measure the agreement between two probabilistic distributions. However, the SIS does not require abundant measurement data to estimate a precise probability density function, which is a clear benefit of the SIS metric in the presence of limited experimental data in practical applications.

Further development of the SIS includes the integration in the updating of nonlinearity systems. Nonlinear updating has been developed as an important branch of model updating. This development is expected to meet the tendency of light-weight and large-deformable structures. Two challenges of nonlinear updating have been identified: 1) it is difficult to obtain a full-field experimental measurement to capture the nonlinearity, especially for large-deformable structures; 2) the nonlinear properties are hard to be updated together with the normal parameters in a uniform framework. For the connection between the nonlinear updating and the proposed SIS UQ metric, since nonlinear updating is still a special case of model updating, it hence still requires a UQ metric to capture the discrepancy between the measured and simulated outputs. The SIS metric focuses on the comparison of outputs, while the nonlinearity relates to the inherent property of structures, i.e. the input parameters. In this sense, the SIS can also be used for nonlinear model updating. To achieve this development, a two-phase updating framework would be developed to calibrate the linear and nonlinear properties separately while with the SIS metric to be integrated into both phases.

A limitation of the SIS metric is that it ignores the correlations feature of multidimensional data. The current treatment is to first marginalize the samples to each dimension, and then calculate the mean of the SIS on all the dimensions. This limitation is similar to that of the Probability-box (P-box) when facing multidimensional data. Future work is expected to extend the SIS metric with dependence description tools, e.g. the Copula function, to enhance the capacity of correlation quantification.

Acknowledgements

This work is supported by the Fundamental Research Funds for the Central Universities (FRF-BD-20-08A, FRF-BD-19-003A), the Fundamental Technical Project (JSZL2020203B001), the Postdoctor Research Foundation of Shunde Graduate School of University of Science and Technology Beijing (2021BH012), and the National Natural Science Function of China (12102036). The third author acknowledges the support of the Research Foundation Flanders (FWO) under grant 12P3519N, as well as of the Alexander von Humboldt Foundation.

References

[1] J.E. Mottershead, M.I. Friswell, Model updating in structural dynamics: A survey, J. Sound Vib. 167 (1993) 347–375. https://doi.org/10.1006/jsvi.1993.1340.

[2] Friswell, I. M., Finite Element Model Updating in Structural Dynamics, Finite element model updating in structural dynamics, n.d.

[3] Y. Govers, H. Haddad Khodaparast, M. Link, J.E. Mottershead, A comparison of two stochastic model updating methods using the DLR AIRMOD test structure, Mech. Syst. Signal Process. 52–53 (2015) 105–114. https://doi.org/10.1016/j.ymssp.2014.06.003.

[4] E. Simoen, G. De Roeck, G. Lombaert, Dealing with uncertainty in model updating for damage assessment: A review, Mech. Syst. Signal Process. (2015). https://doi.org/10.1016/j.ymssp.2014.11.001.

[5] C. Mares, J.E. Mottershead, M.I. Friswell, Stochastic model updating: Part 1-theory and simulated example, Mech. Syst. Signal Process. 20 (2006) 1674–1695. https://doi.org/10.1016/j.ymssp.2005.06.006.

[6] J.E. Mottershead, C. Mares, S. James, M.I. Friswell, Stochastic model updating: Part 2-application to a set of physical structures, Mech. Syst. Signal Process. 20 (2006) 2171–2185. https://doi.org/10.1016/j.ymssp.2005.06.007.

[7] Y. Govers, M. Link, Stochastic model updating-Covariance matrix adjustment from uncertain experimental modal data, Mech. Syst. Signal Process. 24 (2010) 696–706. https://doi.org/10.1016/j.ymssp.2009.10.006.

[8] H.H. Khodaparast, J.E. Mottershead, M.I. Friswell, Perturbation methods for the estimation of parameter variability in stochastic model updating, Mech. Syst. Signal Process. 22 (2008) 1751–1773. https://doi.org/10.1016/j.ymssp.2008.03.001.

[9] J.L. Beck, L.S. Katafygiotis, Updating models and their uncertainties. I: Bayesian statistical framework, J. Eng. Mech. 124 (1998) 455–461. https://doi.org/10.1061/(ASCE)0733-9399(1998)124:4(455).

[10] M.C. Kennedy, A. O'Hagan, Bayesian calibration of computer models, J. R. Stat. Soc. Ser. B (Statistical Methodol. 63 (2001) 425–464. https://doi.org/10.1111/1467-9868.00294.

[11] J.L. Beck, S.K. Au, Bayesian updating of structural models and reliability using Markov chain Monte Carlo simulation, J. Eng. Mech. 128 (2002) 380–391. https://doi.org/10.1061/(ASCE)0733-9399(2002)128:4(380).

[12] J. Ching, Y.C. Chen, Transitional Markov chain Monte Carlo method for Bayesian model updating, model class selection, and model averaging, J. Eng. Mech. 133 (2007) 816–832. https://doi.org/10.1061/(ASCE)0733-9399(2007)133:7(816).

[13] E. Patelli, Y. Govers, M. Broggi, H.M. Gomes, M. Link, J.E. Mottershead, Sensitivity or Bayesian model updating: a comparison of techniques using the DLR AIRMOD test data, Arch. Appl. Mech. 87 (2017) 905–925. https://doi.org/10.1007/s00419-017-1233-1.

[14] A. Lye, A. Cicirello, E. Patelli, Sampling methods for solving Bayesian model updating problems: A tutorial, Mech. Syst. Signal Process. 159 (2021) 107760. https://doi.org/10.1016/j.ymssp.2021.107760.

[15] M. Kitahara, S. Bi, M. Broggi, M. Beer, Nonparametric Bayesian stochastic model updating with hybrid uncertainties, Mech. Syst. Signal Process. 163 (2022) 108195. https://doi.org/10.1016/j.ymssp.2021.108195.

[16] Y. Zhao, Z. Deng, X. Zhang, A robust stochastic model updating method with resampling processing, Mech. Syst. Signal Process. 136 (2020) 106494. https://doi.org/https://doi.org/10.1016/j.ymssp.2019.106494.

[17] L.G. Crespo, S.P. Kenny, Synthetic Validation of Responses to the NASA

Langley Challenge on Optimization under Uncertainty, Mech. Syst. Signal Process. 164 (2022) 108253. https://doi.org/10.1016/J.YMSSP.2021.108253.

[18] A. Gray, A. Wimbush, M. de Angelis, P.O. Hristov, D. Calleja, E. Miralles-Dolz, R. Rocchetta, From inference to design: A comprehensive framework for uncertainty quantification in engineering with limited information, Mech. Syst. Signal Process. 165 (2022) 108210. https://doi.org/10.1016/J.YMSSP.2021.108210.

[19] A. Lye, M. Kitahara, M. Broggi, E. Patelli, Robust optimization of a dynamic Black-box system under severe uncertainty : A distribution-free framework, Mech. Syst. Signal Process. 167 (2022) 108522. https://doi.org/10.1016/j.ymssp.2021.108522.

[20] S. Bi, K. He, Y. Zhao, D. Moens, M. Beer, J. Zhang, Towards the NASA UQ Challenge 2019: Systematically forward and inverse approaches for uncertainty propagation and quantification, Mech. Syst. Signal Process. 165 (2022) 108387. https://doi.org/10.1016/j.ymssp.2021.108387.

[21] S. Bi, S. Prabhu, S. Cogan, S. Atamturktur, Uncertainty quantification metrics with varying statistical information in model calibration and validation, AIAA J. 55 (2017) 3570–3583. https://doi.org/10.2514/1.J055733.

[22] S. Bi, M. Broggi, M. Beer, The role of the Bhattacharyya distance in stochastic model updating, Mech. Syst. Signal Process. 117 (2019) 437–452. https://doi.org/10.1016/j.ymssp.2018.08.017.

[23] S. Bi, M. Beer, J. Zhang, L. Yang, K. He, Optimization or Bayesian Strategy? Performance of the Bhattacharyya Distance in Different Algorithms of Stochastic Model Updating, ASCE-ASME J Risk Uncert Engrg Sys Part B Mech Engrg. 7 (2021). https://doi.org/10.1115/1.4050168.

[24] S. Kullback, R.A. Leibler, On Information and Sufficiency, Ann. Math. Stat. 22 (1951) 79–86. https://doi.org/10.1214/aoms/1177729694.

[25] M. Faes, D. Moens, Recent Trends in the Modeling and Quantification of Non-probabilistic Uncertainty, Arch. Comput. Methods Eng. (2019).

[26] B. Zheng, K. Yu, S. Liu, R. Zhao, Interval model updating using universal grey mathematics and Gaussian process regression model, Mech. Syst. Signal Process. 141 (2020) 106455. https://doi.org/https://doi.org/10.1016/j.ymssp.2019.106455.

[27] D. Moens, M. Hanss, Non-probabilistic finite element analysis for parametric uncertainty treatment in applied mechanics: Recent advances, Finite Elem. Anal. Des. 47 (2011) 4–16. https://doi.org/10.1016/j.finel.2010.07.010.

[28] Y. Zhao, Z. Deng, Y. Han, Dynamic response analysis of structure with hybrid random and interval uncertainties, Chaos, Solitons & Fractals. 131 (2020) 109495. https://doi.org/https://doi.org/10.1016/j.chaos.2019.109495.

[29] M. Faes, J. Cerneels, D. Vandepitte, D. Moens, Identification and quantification of multivariate interval uncertainty in finite element models, Comput. Methods Appl. Mech. Eng. 315 (2017) 896–920. https://doi.org/10.1016/J.CMA.2016.11.023.

[30] M. Faes, M. Broggi, E. Patelli, Y. Govers, J. Mottershead, M. Beer, D. Moens, A multivariate interval approach for inverse uncertainty quantification with limited experimental data, Mech. Syst. Signal Process. 118 (2019) 534–548. https://doi.org/10.1016/j.ymssp.2018.08.050.

[31] H.H. Khodaparast, J.E. Mottershead, K.J. Badcock, Interval model updating with irreducible uncertainty using the Kriging predictor, Mech. Syst. Signal Process. 25 (2011) 1204–1226. https://doi.org/10.1016/j.ymssp.2010.10.009.

[32] S.-E. Fang, Q.-H. Zhang, W.-X. Ren, An interval model updating strategy using interval response surface models, Mech. Syst. Signal Process. 60–61 (2015) 909–927.

[33] R. Callens, M. Faes, D. Moens, Multilevel Quasi-Monte Carlo For Interval Analysis, Int. J. Uncertain. Quantif. 12 (2021) 1–15.

[34] Z. Deng, Z. Guo, Interval identification of structural parameters using interval overlap ratio and Monte Carlo simulation, Adv. Eng. Softw. 121 (2018) 120–130. https://doi.org/10.1016/J.ADVENGSOFT.2018.04.006.

[35] C. Jiang, X. Han, G.R. Liu, Optimization of structures with uncertain constraints based on convex model and satisfaction degree of interval, Comput. Methods Appl. Mech. Eng. 196 (2007) 4791–4800. https://doi.org/https://doi.org/10.1016/j.cma.2007.03.024.

[36] Y. Wang, L. Sui, Design of experiment and matlab data analysis, Tsinghua University Press, Beijing, 2012.

[37] J.E. Mottershead, M. Link, M.I. Friswell, The sensitivity method in finite element model updating: A tutorial, Mech. Syst. Signal Process. 25 (2011) 2275–2296. https://doi.org/10.1016/j.ymssp.2010.10.012.